

Global Minima Search for Sodium- and Magnesium-Adsorbed Polymorphic Borophene

Vaishnavi Vishnubhotla, Arnab Kabiraj, Aninda J. Bhattacharyya, and Santanu Mahapatra*

Cite This: <https://doi.org/10.1021/acs.jpcc.2c02727>

Read Online

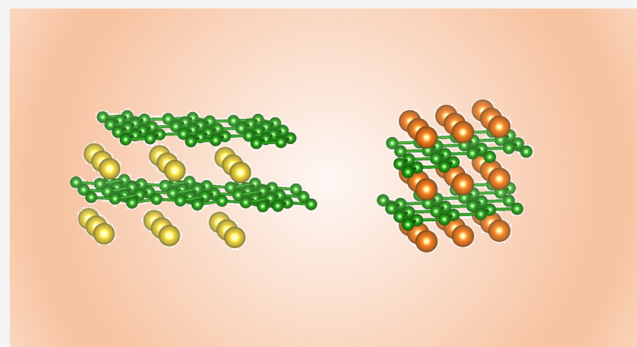
ACCESS |

Metrics & More

Article Recommendations

Supporting Information

ABSTRACT: Monolayer allotropes of boron (borophene) are being explored extensively for alkali-ion battery anode materials due to their metallicity and ultralow molar mass. However, the inherited polymorphism of borophene has made the alkali-ion adsorption mechanisms abstruse. Previous computational studies rely on the uniform-adsorption model, which fails to capture the adsorption-induced phase change in borophene and thus predicts nonrealistic values of the specific capacity. Here, we employ ab initio global-minima-search techniques to gain atomistic insights into the polymorphism-driven sodium- and magnesium-ion binding process. Our well-designed computational method combines two different search techniques. It reveals different nonidealities (e.g., bond cleavage, electroplating, phase transition, etc.), which may assist the future experimental efforts on polymorphic borophene. In contrast to earlier reports, our study finds borophene to be an outstanding candidate for Mg-ion batteries (specific capacity of 3648.54 mAh/g) but not so promising for Na storage due to relatively high formation energies (+0.09 eV/atom) of Na-B compounds and phase deformation upon adsorption.



INTRODUCTION

Lithium-ion batteries (LIBs) are one of the most advanced battery technologies because of their higher efficiency toward energy conversion and storage and commercial viability. High power and energy densities, as well as the long cycle and shelf life of LIBs, are other advantages.¹ To meet the requirements of high-power tools and electric vehicles, electrode materials with high Li reversible storage capacity and fast electron transport are needed for lithium-ion batteries.² The choice of the anode material is essential as the battery's performance depends on the chemistry of the electrode material. The monolayer of boron, commonly known as borophene, has appeared as a promising anode material for high-capacity batteries since its metallicity, ultralight weight, and high surface-to-mass ratio might yield significant enhancement in the specific capacity of the electrode. Polymorphism is an inherent property of borophene, and the energy difference between different phases was found to be mostly small.³ The striped phase of borophene was first reported in late 2015. It was synthesized under ultrahigh vacuum conditions on an Ag(111) substrate.⁴ The honeycomb structure, which is energetically unfavorable to other metallic phases, was synthesized later on the Al(111) substrate.⁵ While the charge transfer from the Ag substrate is negligible, Al can donate nearly one electron to each boron atom, enabling the construction of a honeycomb structure just like graphene.^{5,6} The striped phase has a triangular arrangement of boron atoms with a buckled and highly anisotropic structure. β_{12} and χ_3 phases, on the other hand, are flat structures containing line defects of hexagonal

holes. The structure of borophene could be viewed as a $B_{1-x}V_x$ pseudo-alloy, where x denotes the vacancy density.^{3,7} The corresponding x values for β_{12} and χ_3 borophenes are 1/6 and 1/5, respectively. The stability of the borophene structure depends on the vacancy density (V) and the substrate material. The most stable structures are in the range of $x = 0.1-0.15$, making it possible to synthesize mixed-phase samples instead of single-phase ones for better performance.³ Theoretical studies^{8,9} tout borophene as an exceptional candidate for Li-ion battery anodes because of its unique morphology and metallic characteristics. However, due to the extremely high demand, Li, dubbed "the new oil," is becoming increasingly costly.¹⁰ To reduce the battery production cost, in recent times, other alkali metals, e.g., sodium and magnesium, are also being explored as alternatives to lithium because of their abundance in nature¹¹ and the two-electron donation process of Mg, which can enhance the specific capacity significantly. However, sodium- and magnesium-ion batteries generally exhibit low energy capacity, which can be improved by replacing conventional electrode materials with borophene. First-principles-based investigation using density

Received: April 20, 2022

Revised: April 27, 2022

functional theory (DFT) has been a common route to estimate the essential figure of merits (FOMs) of two-dimensional (2D) materials as potential alkali-ion battery electrodes,^{12,13} which can act as useful guidelines for future experimental endeavors. These studies also provide chemical insights into the adsorbate binding at the atomic limit, which is difficult to probe even with a sophisticated experimental setup. However, most of these efforts rely on a computationally economic “uniform-adsorption” model, which most of the time is not guaranteed to result in the ionic ground state.^{14–18} More rigorous approaches^{19,20} involving “global minima search” techniques have demonstrated that the uniform-adsorption model predicts nonrealistic values of the specific capacity of any anode material since it cannot capture the cleavage and restoration of chemical bonds during the lithiation and delithiation process. A recent study⁹ also demonstrated the necessity of the global minima search technique for polymorphism-dominated materials (like borophene) to capture the adsorbate-induced phase changes.

In this work, we investigate the potential of borophene allotropes as anode materials for sodium- and magnesium-ion batteries. While other earth-abundant alkali metals such as potassium, aluminum, and calcium seem attractive prospects as well, they are not explored in this paper because of the following reasons. For K and Ca, even the lightest available pseudopotential has seven and eight valence electrons, respectively, which imposes a restrictive computational budget on a high-throughput study like ours. On the other hand, there is a light (three electrons) pseudopotential available for Al, but multiple previous studies have shown that the charge transfer from the Al ion to the adsorbent is even less than that of the Mg ion, rendering Al-ion batteries low-capacity and unsuitable for our study.^{21,22} We assess the thermodynamic suitability of cation-borophene compounds by combining a bottom-up evolutionary structure-searching and a top-down random structure-searching algorithm. While a monolayer of boron has been demonstrated as an excellent candidate for lithium-ion storage,⁹ we find that the results are less promising for sodium-ion storage due to the relatively high formation energies and phase deformation upon adsorption in contrast to previous studies.²³ However, the monolayer honeycomb phase of borophene was found to be a highly reliable anode material for magnesium-ion storage with good formation energy (−0.14 eV/atom) and high specific capacity (3648.54 mAh/g) at the composition ratio of 0.5.

■ COMPUTATIONAL DETAILS

Geometry relaxations were carried out using the Vienna ab initio simulation package (VASP)^{24–27} with the projector-augmented wave (PAW)²⁸ method and the generalized gradient approximation-Perdew–Burke–Ernzenhof (GGA-PBE)²⁹ exchange–correlation functional. The valence electrons that are expanded in plane-wave basis sets are as follows: B, $2s^2 2p^1$; Na, $3s^1$; and Mg, $3s^2$. The cutoff energy of 450 eV was used for the plane-wave basis sets to avoid any Pulay stress. For all structural relaxations, $a > \frac{30}{a} \times \frac{30}{b} \times 1$ γ -centered k -point grid was used to sample the Brillouin zone, where a and b are the lengths of the in-plane lattice parameters of the particular supercell in Å. $A > \frac{60}{a} \times \frac{60}{b} \times 1$ similar k -mesh was used for all static runs. Electronic convergence was set to be attained when the difference in energy of successive electronic steps became less than 10^{-6} eV, whereas the structural geometry was optimized until the maximum Hellmann–Feynman force on every atom fell below 0.01 eV/Å. An ample vacuum space of more than 20 Å

in the direction of c was applied to avoid any spurious interaction between periodically repeated layers. Semiempirical dispersion corrections with the DFT-D3 method as developed by Grimme³⁰ were used in all of the calculations.

While finding the energetically most favorable single Na-/Mg-ion-adsorbed borophene structure is simple, it is highly nontrivial to find the same for multiple ion adsorption. In the literature,^{31–33} it is commonly executed using the “uniform-adsorption model” since it is computationally economical. However, such a model does not assure ground-state configuration and thus often predicts nonrealistic values of specific capacity. To assess the realistic reversible specific capacity here, we combine the bottom-up and top-down structure-search techniques. To search for the most stable adsorbed phases globally, we calculated the formation energy of sodium- and magnesium-adsorbed borophene electrode compounds as a function of adsorbate concentration and subsequently constructed the convex hull. The convex hull’s construction was achieved through a bottom-up approach, starting with random atomic configurations of Na/Mg and ultrathin boron and then exploring possible stable adsorbed phases through an evolutionary algorithm. Such a convex hull may be used as a guideline for experimentalists that allow drawing a fair comparison of the thermodynamic stability of different sodium- and magnesium-adsorbed 2D borophene phases in terms of both adsorbate concentration and polymorphism, making it easier to synthesize and test these systems. Bottom-up structure searching for the most stable structures in the composition space of Na_xB_y and Mg_xB_y is performed using the Universal Structure Predictor: Evolutionary Xtallography (USPEX)^{34–36} code interfaced with VASP. This is based on an evolutionary algorithm featuring local optimization, real-space representation, and flexible physically motivated variation operators.⁹ The number of atoms in each structure is kept between 2 and 12 to limit the computational budget as many structures need to be explored for each configuration. After relaxation, only structures with thickness less than 6.5 Å are considered; the thicker structures are assigned high positive energy, and their generation is contained. The thickness constraint is determined by doing several test runs. The system performs sophisticated genetic operations on the previous generation’s best systems to obtain the next generations, which are a combination of random and inherited structures. The search is continued until ten consecutive generations produce the same results.

We conduct a top-down structure search for larger supercells using the ab initio random structure-searching (AIRSS) algorithm.³⁷ It begins with an individual phase and predicts the most stable structure at a particular adsorbate concentration, which is often found to be not a uniformly adsorbed but a severely deformed system.²² A many-atom top-down structure search can be used to find the precise local minima after a bottom-up search with a small number of atoms has yielded an approximation of the global minimum. In the top-down approach, Na and Mg ions are placed randomly on the adsorbent supercell using the AIRSS initial configuration generation engine, and then, they are relaxed to the nearest local minima. A γ -point-only k -mesh is used for structure relaxation while searching for the lowest energy phases. The top-five lowest energy structures from every energy-rank list are processed using the above-mentioned denser k -mesh structural relaxation, and then, static runs are performed on the most stable structure. In addition to this, to assess the thermal stability of the

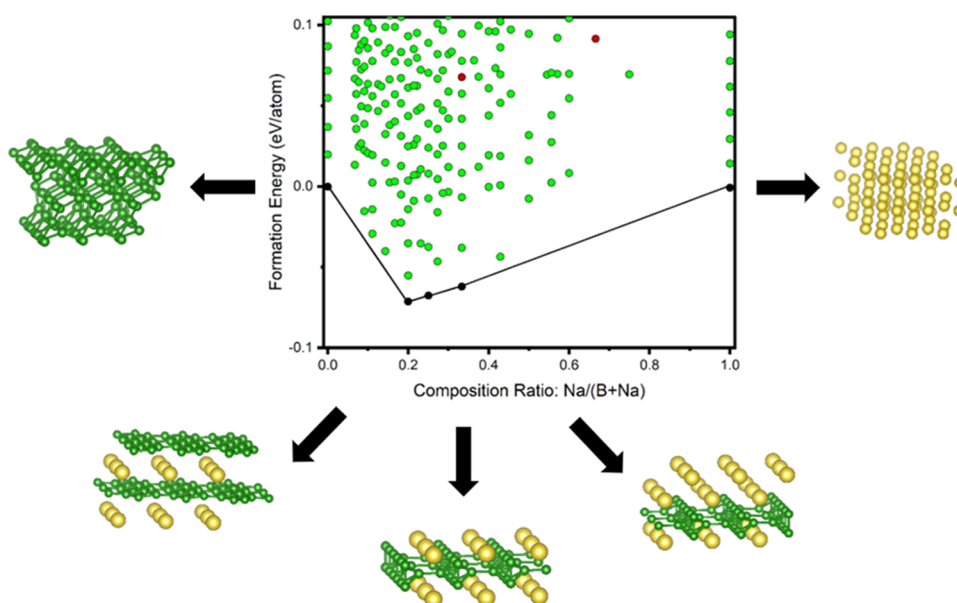


Figure 1. Bottom-up evolutionary structure-search-constructed convex hull for the Na_xB_y composition space in the 2D limit along the most stable crystal structures. The green and yellow balls represent B and Na atoms, respectively. The plot points marked red indicate the structures that are manually constructed.

AIRSS-found most stable phases, we perform ab initio molecular dynamics (AIMD) studies. To perform AIMD simulations on 135–144 atom supercells with minimal temperature fluctuations, a canonical ensemble (NVT) is used with a 2 fs time step, and a Nosé–Hoover thermostat^{38,39} is employed with a γ -point-only k -point sampling for the intermediate DFT calculations. The density-derived electrostatic and chemical (DDEC) atomic charge analysis is performed with charge densities from DFT static runs as inputs to find the amount of charge transfer for various processes.^{40–43} All of the crystal structures are visualized using the tool VESTA.⁴⁴

We calculate the formation energy using the following equation:

$$E_{\text{form}} = \frac{E_{\text{A}_x\text{B}_y} - xE_{\text{Aphase}} - yE_{\text{Bphase}}}{x + y} \quad (1)$$

A refers to the adsorbate, which is either Na or Mg, and B refers to the adsorbent, which is a Borophene phase in our work. $E_{\text{A}_x\text{B}_y}$ is the total energy of the A_xB_y system and E_{Aphase} and E_{Bphase} are the per atom total energies of the most stable A and B phases found in the evolutionary search for a specific A_xB_y system in the 2D limit. x and y are integers.

The cohesive energy is calculated as

$$E_{\text{coh}} = \frac{E_{\text{A}_x\text{B}_y} - xE_{\text{Aatom}} - yE_{\text{Batom}}}{x + y} \quad (2)$$

E_{Aatom} and E_{Batom} are the isolated atom energies of the adsorbate and boron atoms, respectively.

The adsorption energy is calculated as

$$E_{\text{ads}} = \frac{E_{\text{A}_x\text{B}_y} - x\mu_{\text{A}} - yE_{\text{B}_y}}{x} \quad (3)$$

Here, μ_{A} is the chemical potential of Na or Mg. E_{B_y} is the energy of the adsorbent phase before Na or Mg adsorption. For calculating the chemical potential, the metallic bulk phase is taken as a reference as it is a more reliable reference state compared to the neutral atom in the gas phase. Chemical

potential that is calculated using the metallic bulk state as a reference directly compares the resulting adsorption energy with the metal's bulk cohesive energy, therefore providing more physical insights such as the possibility of clustering.⁴⁵ In terms of formation, adsorption, and cohesive energies, lower energy implies more stable structures. Positive adsorption energy indicates the possibility of clustering and phase separation with the substrate instead of adsorption.

The specific capacity in mAh/g can be calculated using

$$C = \frac{\nu F f_{\text{max}} \cdot 10^3}{M} \quad (4)$$

where f_{max} is the maximum Na or Mg concentration adsorbed per formula unit of the substrate. M is the molar weight of the adsorbent. $F = 26.801$ Ah/mol is the Faraday constant, and ν is the charge transferred obtained by performing DDEC atomic charge analysis.^{40–43}

We also calculate the average open circuit voltage (OCV) using the following equation

$$\text{OCV} \approx - \frac{[E_{\text{A}_{f_{\text{max}}}\text{B}} - E_{\text{A}_{f_{\text{min}}}\text{B}} - (f_{\text{max}} - f_{\text{min}}) \mu_{\text{A}}]}{(f_{\text{max}} - f_{\text{min}})e} \quad (5)$$

where f_{max} and f_{min} are maximum and minimum Na or Mg concentration adsorbed per formula unit of the substrate, respectively. Here, $f_{\text{min}} = 0$ for all of the cases, whereas f_{max} depends on the composition ratio of the structure.

RESULTS AND DISCUSSION

We perform calculations on the four experimentally synthesized phases of borophene: β_{12} , χ_3 , striped, and honeycomb.^{4,46} The structures that are not obtained from the convex hull are manually constructed, starting with a standard phase of borophene and adding sodium and magnesium atoms with different composition ratios. These structures are compared in terms of their formation energies to obtain the most stable structure for a particular adsorbed phase of borophene.

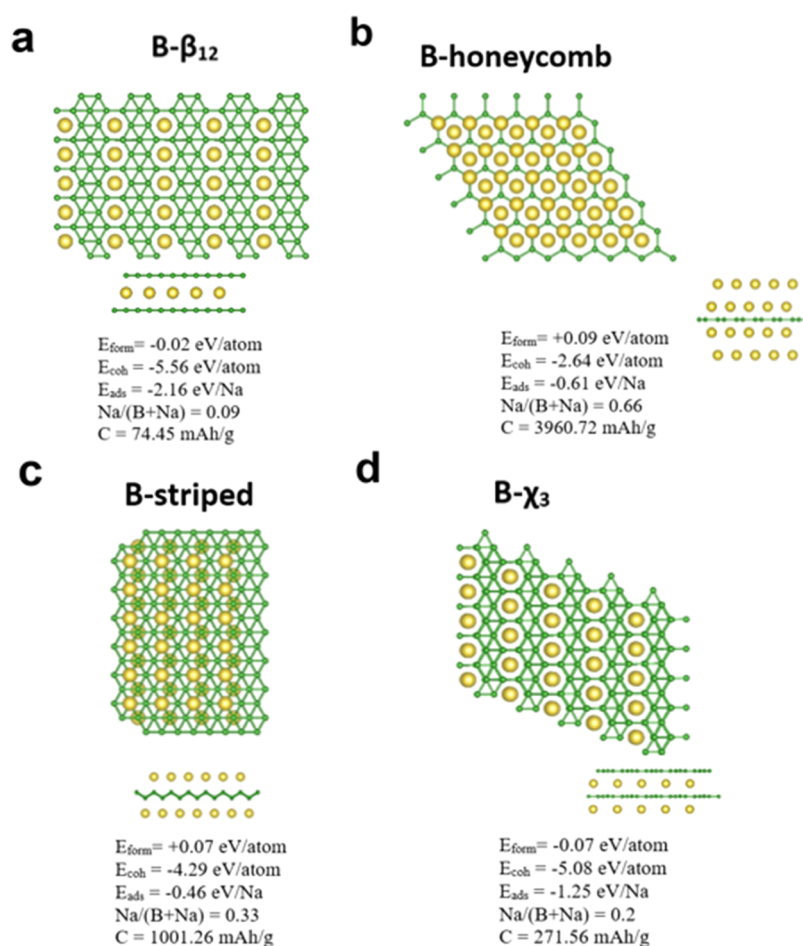


Figure 2. Top and side views of borophene allotropes and their most stable Na-adsorbed phases found in the bottom-up evolutionary structure-searching approach with relevant energies and estimated storage capacities for β_{12} , honeycomb, striped, and χ_3 phases are shown in parts (a), (b), (c), and (d), respectively. Striped and honeycomb phases are manually constructed. Specific capacity values are calculated using the charge transferred obtained from DDEC analysis. The green and yellow balls represent B and Na atoms, respectively.

Sodium-Adsorbed Borophene. The evolutionary search-constructed convex hull along with the most stable Na-adsorbed borophene structures is depicted in Figure 1. It is difficult to link the most stable pristine 2D-B (leftmost) to a bulk phase due to the high polymorphism of bulk boron and substantial surface rebuilding in the 2D limit. According to the convex hull in Figure 1, the global minimum for the Na-adsorbed borophene structure is at the composition ratio $\text{Na}/(\text{B} + \text{Na}) = 0.2$, which corresponds to two layers of the Na-intercalated bilayer χ_3 phase. This structure, however, has a specific capacity of 271.56 mAh/g, which is less compared to the specific capacity of other synthesized borophene phases.

The global minimum of the convex hull occurs at composition ratio 0.2. Initially, the formation energy becomes more negative as the composition ratio increases. This is because as the adsorbate concentration increases, it introduces deformation in the substrate and facilitates Na-ion binding. As the composition ratio increases beyond the global minima, the repulsion between Na ions becomes a major factor and the formation energy gradually increases to zero.

The amount of charge transferred from Na atoms to each boron atom is calculated from DDEC atomic charge analysis. The net atomic charges obtained from DDEC analysis are simultaneously optimized to reproduce chemical states of atoms and the electrostatic potential.^{40–43} The structures depicting the

charge density difference are shown in Figure S1. Along with synthesized phases, we have also shown the charge density difference in the new structure obtained from the convex hull in part (e) of Figure S1. The charge transferred is calculated by taking the average of charge contribution of all of the sodium atoms. These values of charge transferred are used to calculate the specific capacities of all of the structures shown in Figure 2. The ideal values of specific capacities and the values calculated using the charge transferred obtained from DDEC analysis are given in Table 1. Evidently, incorporating the charge transfer nonideality reduces the estimated values of the specific capacity quite a bit compared to their ideal values. In addition to this, the

Table 1. Amount of Charge Transferred and Corresponding Specific Capacity Values in Comparison with Ideal Values of Specific Capacity for Different Na-Adsorbed Phases of Borophene Obtained through the Bottom-Up Structure-Search Approach

borophene phase	ν_{DDEC}	C_{ideal} (in mAh/g)	C_{DDEC} (in mAh/g)	OCV (in V)
β_{12}	0.3	247.93	74.45	2.16
honeycomb	0.79	4958.56	3960.72	0.61
striped	0.81	1239.64	1001.26	0.46
χ_3	0.44	619.82	271.56	1.25

total density of states and the projected density of states for individual orbitals are plotted, and it is observed that there is strong hybridization between s and p orbitals of the sodium atom and the p orbital of the boron atom. The plot of density of states for the most stable Na-adsorbed bilayer χ_3 borophene phase is shown in Figure S2.

Spin polarization calculations have been performed on all of the structures and it has been observed that the non-spin-polarized structures are more stable in all cases. Hence, these structures are considered for calculation of other energy parameters. The honeycomb phase shows the highest specific capacity (3960.72 mAh/g) among the Na-adsorbed borophene structures, but it is not the most stable structure due to its relatively high formation energy. This phase is manually obtained by adding Na atoms to a single unit cell of honeycomb-phase borophene to find the least adsorption energy at a composition ratio of $\text{Na}/(\text{B} + \text{Na}) = 0.66$. It can be observed that the charge transferred for β_{12} and χ_3 phases is much less than the ideal charge of one electron, resulting in lower values of specific capacities. The striped Na-adsorbed phase is constructed by taking a 2×2 striped borophene supercell and adding Na atoms to obtain the structure with the least formation energy. It is important to note that the size of the supercell is limited because we are keeping the total number of atoms in the structure between 2 and 12. Na atoms are placed on different adsorption sites, and ionic relaxations followed by energy calculations are performed to find the most stable structure. The β_{12} phase is obtained from the convex hull at a composition ratio of 0.09. It has good adsorption energy but very less specific capacity (74.45 mAh/g) and is therefore not ideal for an anode material.

From the convex hull in Figure 1, we can observe that the most stable monolayer Na-adsorbed borophene structure is obtained at $\text{Na}/(\text{B} + \text{Na}) = 0.33$. An AIRSS-based top-down study is performed at the same Na concentration for all of the synthesized phases of borophene. As mentioned before, the charge transferred to boron atoms is calculated through DDEC atomic charge analysis, and this charge is used to calculate specific capacity values. These values are given in Table 2. It

Table 2. Amount of Charge Transferred and Corresponding Specific Capacity Values in Comparison with Ideal Values of Specific Capacity for Different Na-Adsorbed Phases of Borophene Obtained through the Top-Down AIRSS Approach

borophene phase	ν_{DDEC}	C_{ideal} (in mAh/g)	C_{DDEC} (in mAh/g)	OCV (in V)
β_{12}	0.66	1239.64	818.13	0.73
honeycomb	0.65	1239.64	803.11	2.37
striped	0.76	1239.64	946.45	0.7
χ_3	0.66	1239.64	817.68	0.65

should be noted that significant structural deformations or high formation energies are observed in Figure 3. Charge density difference for the structures obtained through AIRSS is demonstrated in Figure S3.

Na-adsorbed honeycomb borophene has the least adsorption energy of $E_{\text{ads}} = -2.368$ eV/Na and a specific capacity of 803.11 mAh/g. This value of adsorption energy is large enough for sodium-borophene stability during the adsorption process. The other phases have relatively less negative values of adsorption energy, indicating less adsorption-stability compared to the

honeycomb phase. The Na-adsorbed striped phase has the highest amount of charge transferred and thereby the highest specific capacity of 946.45 mAh/g compared to other phases, but the structure is less stable due to the relatively higher formation energy. However, we can observe in Figure 3 that all of the phases undergo deformation upon Na adsorption unlike the structures obtained using evolutionary search.

It has already been demonstrated that honeycomb borophene is an excellent candidate for Li-ion storage with good formation energy and a high specific capacity of 2479.28 mAh/g.⁹ However, this is not the case for Na-ion storage. From the bottom-up approach, we get a maximum specific capacity of 3960.72 mAh/g at a concentration of 0.66 for the manually constructed honeycomb phase; however, the relatively high formation energy (+0.09 eV/atom) is making the structure unlikely to exist. The most stable structure obtained from the convex hull corresponds to the bilayer χ_3 phase, with a low specific capacity (271.56 mAh/g). Now, from the top-down AIRSS study, we find the monolayer β_{12} phase to be the most stable structure with the lowest formation energy (−0.05 eV/atom). At the same time, we observe that the structure is irreversibly damaged at a concentration of 0.33. Therefore, the specific capacity value is bound to be lower than 818.13 mAh/g for the monolayer. However, a specific capacity of 1860 mAh/g has been reported for monolayer borophene (honeycomb phase) using a uniform-adsorption model in a previous study,¹⁴ which is much higher than our prediction. Thus, we can conclude that borophene is not a promising candidate as an anode material for sodium-ion storage even though it has a low diffusion barrier and high electronic conductivity as demonstrated in a previous study.²³

Magnesium-Adsorbed Borophene. The convex hull along with thermodynamically stable Mg-adsorbed borophene structures is shown in Figure 4. The most stable structure obtained from the convex hull at a composition ratio of $\text{Mg}/(\text{B} + \text{Mg}) = 0.429$ corresponds to the bilayer honeycomb phase. It also has a high specific capacity of 2220.19 mAh/g.

As mentioned before, the honeycomb phase is the most unstable borophene in the pristine form, but charge transfer from the substrate stabilizes this structure. Similar to this mechanism, adsorption of the Mg atoms transfers 1.2 electrons to each boron atom, stabilizing the structure. The charge transferred is obtained from DDEC atomic charge analysis by taking the average of the charge contribution of all of the Mg atoms. Specific capacities are then calculated using the transferred charge obtained by this method. These values, along with the amount of charge transferred and the average open circuit voltage values, are given in Table 3. The structures depicting the charge density difference are shown in Figure S4. Along with synthesized phases, we have also shown the charge density difference in the new structure obtained from the convex hull in part (e) of Figure S4. Total density of states and projected density of states for individual orbitals for the most stable Mg-adsorbed bilayer honeycomb phase are plotted, and it is observed that there is strong hybridization between s and p orbitals of the magnesium atom and the p orbital of the boron atom. This plot of density of states is shown in Figure S5.

Striped and β_{12} phases are not found in the evolutionary search structures so they are manually constructed starting with the standard phases to find the most stable adsorbed structures for each phase. Striped-phase borophene is taken as a 2×2 supercell, and Mg atoms are added to find the most stable structure for that phase at a composition ratio of 0.33.

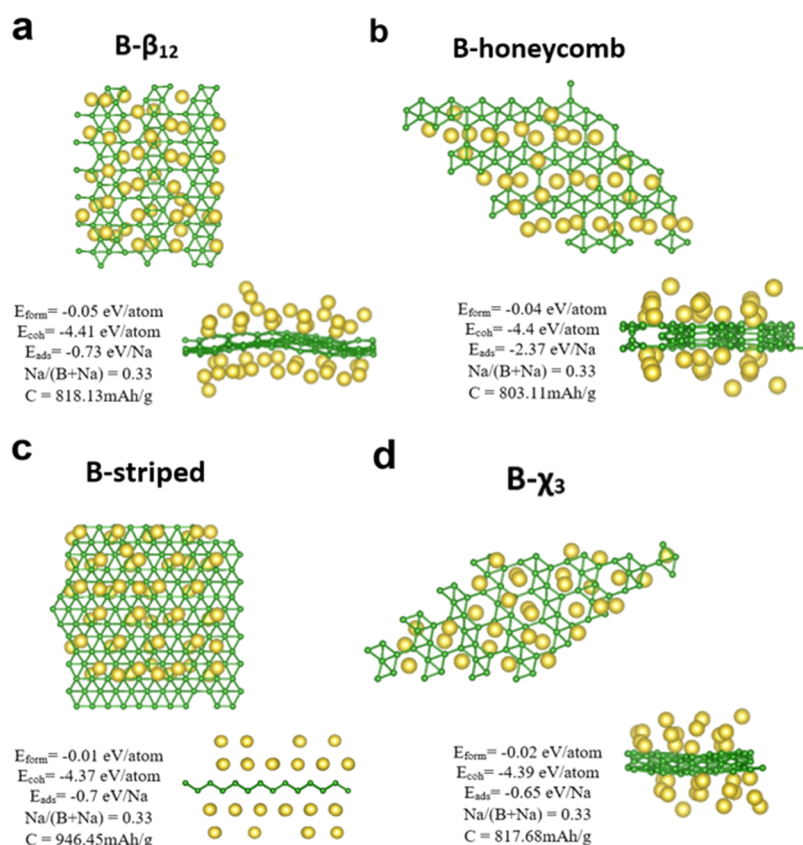


Figure 3. Top and side views of the most stable Na-adsorbed β_{12} , honeycomb, striped, and χ_3 phases of borophene found by the top-down AIRSS approach with relevant energy and concentration parameters are shown in parts (a), (b), (c), and (d), respectively. Specific capacity values are calculated using the charge transferred obtained from DDEC analysis. The green and yellow balls represent B and Na atoms, respectively.

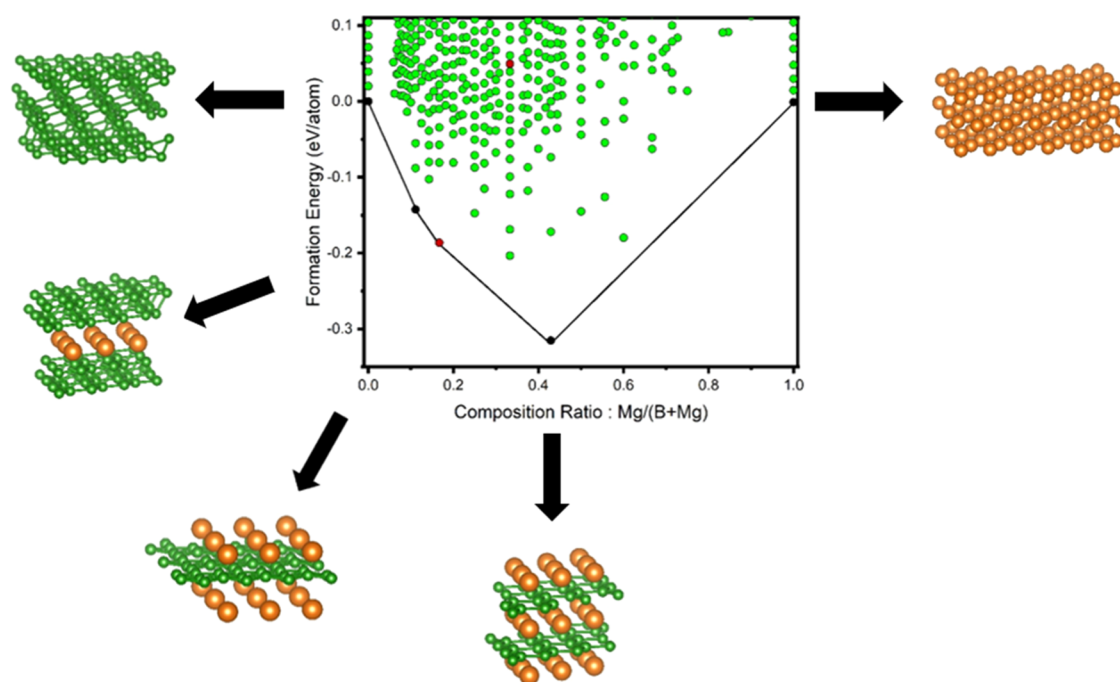


Figure 4. Bottom-up evolutionary structure-search-constructed convex hull for Mg_xB_y composition space in the 2D limit along the most stable crystal structures. The green and orange balls represent B and Mg atoms, respectively. The plot points marked red indicate the structures that are manually constructed.

The striped phase has a good specific capacity of 2220.64 mAh/g, but it has a relatively high formation energy and hence is

not considered the most stable borophene phase for Mg adsorption. It is interesting to note that the most stable Mg-

Table 3. Amount of Charge Transferred and Corresponding Specific Capacity Values in Comparison with Ideal Values of Specific Capacity for Different Mg-Adsorbed Phases of Borophene Obtained through the Bottom-Up Structure-Search Approach

borophene phase	ν_{DDEC}	C_{ideal} (in mAh/g)	C_{DDEC} (in mAh/g)	OCV (in V)
β_{12}	1.6	991.71	795.55	1.94
honeycomb	1.2	3718.92	2220.19	2.03
striped	1.8	2479.28	2220.64	0.23
χ_3	0.97	619.82	302.103	2.05

adsorbed β_{12} phase obtained at a composition ratio of 0.167 falls on the convex hull, as shown in Figure 4. However, this structure has a relatively low specific capacity (795.55 mAh/g). From Figure 5a, it can be seen that the most stable adsorption site for β_{12} borophene is the hexagonal center. This is verified for other phases as well by calculating the formation energies for different structures obtained by placing Mg atoms on all possible adsorption sites. This process is repeated for all experimentally synthesized phases of borophene.

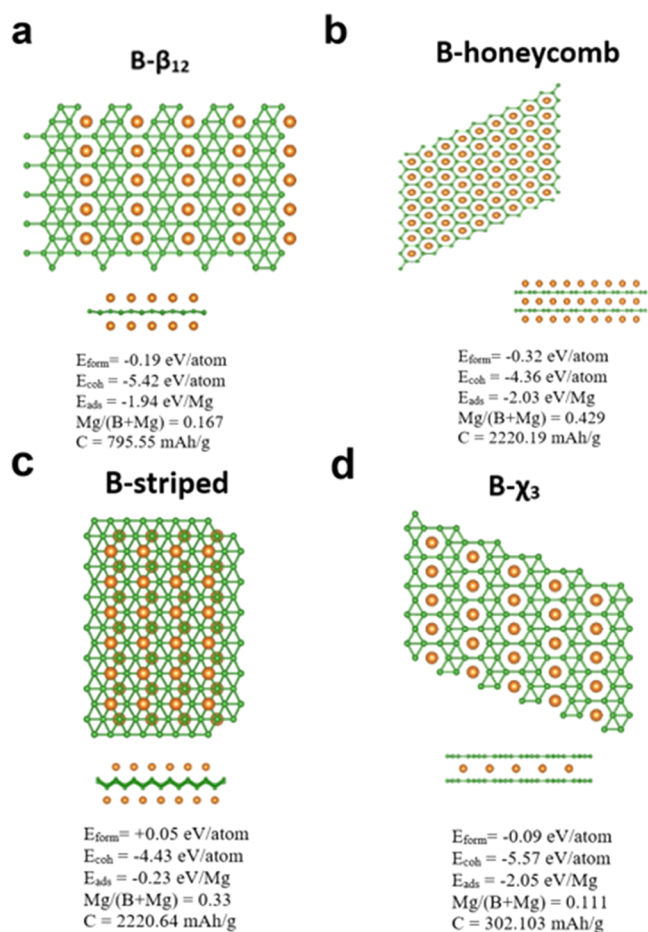


Figure 5. Top and side views of borophene allotropes and their most stable Mg-adsorbed phases found in the bottom-up evolutionary structure-searching approach with relevant energies and estimated storage capacities for β_{12} , honeycomb, striped, and χ_3 phases are shown in parts (a), (b), (c), and (d), respectively. Striped and β_{12} phases are manually constructed. Specific capacity values are calculated using the charge transferred obtained from DDEC analysis. The green and orange balls represent B and Mg atoms, respectively.

AIRSS is performed on all four synthesized phases of borophene with a consistent composition ratio of $\text{Mg}/(\text{B} + \text{Mg}) = 0.5$. In the top-down approach, the composition ratio is fixed from the global minima of the convex hull and the behavior of different phases of Mg-adsorbed borophene at this composition ratio is studied to obtain the most stable phase that can be used as the anode material. The most stable structures obtained through AIRSS along with relevant energy parameters and specific capacity values are shown in Figure 6. The specific capacity values calculated using the charge transferred obtained from DDEC analysis in comparison with the ideal values, the charge transferred, and the average open circuit voltage values are given in Table 4. Charge density difference for the structures obtained through AIRSS is demonstrated in Figure S6.

It can be observed that the uniformly adsorbed monolayer honeycomb borophene phase is the most stable structure for Mg adsorption from AIRSS. The monolayer honeycomb structure has the least formation energy, and the structure also is completely undeformed. This is important as the suitability of the structure as an anode material also depends on its ability to return to the pristine crystal structure upon desorption. The bottom-up structure search also gives the most stable structure for Mg adsorption to be a honeycomb phase, but it is bilayer honeycomb as can be observed from the convex hull in Figure 4.

Except for the striped phase, all of the other phases have hexagonal holes, which are the most stable adsorption sites because of the local electron deficiency of this region. In AIRSS for Mg-adsorbed structures, we observe that the striped borophene phase undergoes partial phase change to the hexagonal phase, and it opens up hexagonal holes as shown in Figure 7.

This indicates the movement of the adsorbed structure toward the global minima, which is the honeycomb phase in this case. It can be seen in Figure 7 that dendrites have started to form in the adsorbed structure at this concentration, making it impractical as an anode material. However, this is just a proof of concept that our methodology captures the movement of the adsorbed structure toward global minima as such an observation was not made in any previous studies^{31–33} that adopted the conventional uniform-adsorption model. Our methodology that combines two approaches captures such events, which are expected to be observed in experiments. The striped phase has the highest specific capacity of 4443.14 mAh/g because of charge transfer of 1.8 electrons to each boron atom, which is the closest to the ideal value of two electrons. Previous works using the uniform-adsorption model reported a specific capacity of 1960 mAh/g for the striped phase of borophene upon Mg adsorption.¹⁶

To assess the thermal stability of the most stable Mg-adsorbed monolayer honeycomb structure found using AIRSS, we performed AIMD simulation. The structure is heated from a temperature of 10–300 K for 10 ps and then subjected to a constant temperature of 300 K for another 10 ps. It has been observed that there is no significant structural distortion confirming the thermal stability of the structure. The snapshots of the structure after the AIMD run are shown in Figure S7.

In summary, bilayer honeycomb-phase borophene is found to be the most stable phase for Mg-ion storage from an evolutionary structure search with a high specific capacity of 2220.19 mAh/g at a composition ratio of 0.429. The top-down AIRSS approach also gives the most stable phase as an undeformed and uniformly adsorbed monolayer honeycomb

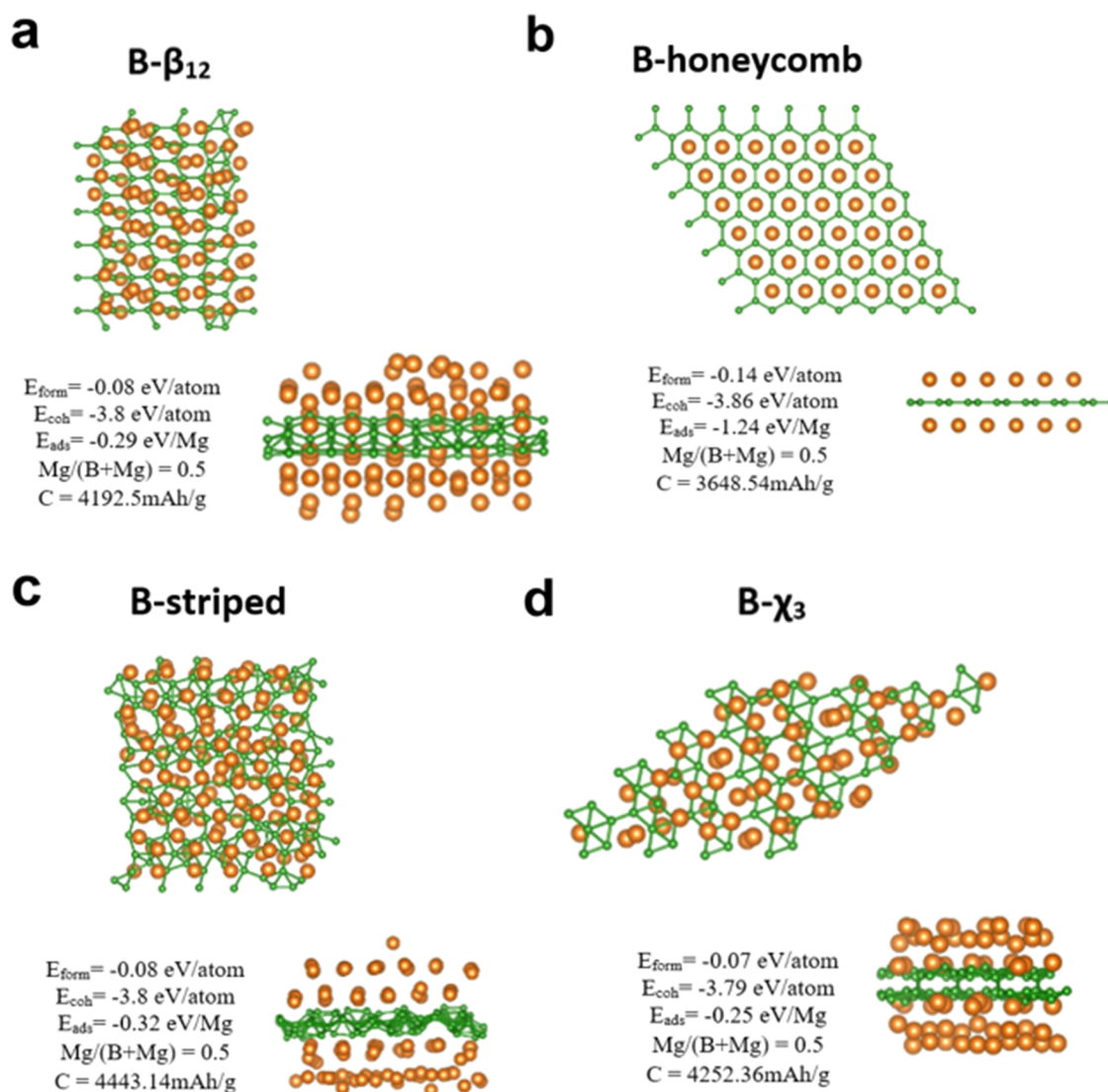


Figure 6. Top and side views of the most stable Mg-adsorbed β_{12} , honeycomb, striped, and χ_3 phases of borophene found by the top-down AIRSS approach with relevant energy and concentration parameters are shown in parts (a), (b), (c), and (d), respectively. Specific capacity values are calculated using the charge transferred obtained from DDEC analysis. The green and orange balls represent B and Mg atoms, respectively.

Table 4. Amount of Charge Transferred and Corresponding Specific Capacity Values in Comparison with Ideal Values of Specific Capacity for Different Mg-Adsorbed Phases of Borophene Obtained through the Top-Down AIRSS Approach

borophene phase	ν_{DDEC}	C_{ideal} (in mAh/g)	C_{DDEC} (in mAh/g)	OCV (in V)
β_{12}	1.7	4958.56	4192.5	0.29
honeycomb	1.5	4958.56	3648.54	1.24
striped	1.8	4958.56	4443.14	0.32
χ_3	1.7	4958.56	4252.36	0.25

phase with a charge transfer of 1.5 electrons to each boron atom and a specific capacity of 3648.54 mAh/g. Therefore, borophene could be a strong candidate as an electrode material for Mg-ion batteries.

CONCLUSIONS

First-principles-calculations-based global minima search was conducted to explore the potential of borophene as an anode

material in sodium- and magnesium-ion batteries. It is found that borophene in the monolayer honeycomb phase is a better candidate as an anode material for Mg-ion storage compared to Na- and Li-ion storage with good specific capacity (3648.54 mAh/g) and less formation energy. These energetics-driven predictions of the storage capacity of sodium and magnesium for different polymorphs of borophene are more realistic than the uniform-adsorption-based predictions. Also, Mg adsorption-driven phase change of the striped phase toward a more stable honeycomb phase is captured in our study. As the Mg-adsorbed honeycomb phase turns out to be the global minima of the Mg-B composition space, we expect other synthesized phases to also undergo phase transition toward the honeycomb phase with repeated charge/discharge cycles. Moreover, the inherent polymorphism of the borophene might result in synthesis of mixed-phased samples instead of purely single-phased samples, where our findings, which provide a global perspective, become extremely useful. The proposed methodology should be as efficient and reliable in predicting the energy-warranted fundamental limit of adsorbate storage capacity even in these complex instances. Our study could therefore act as an

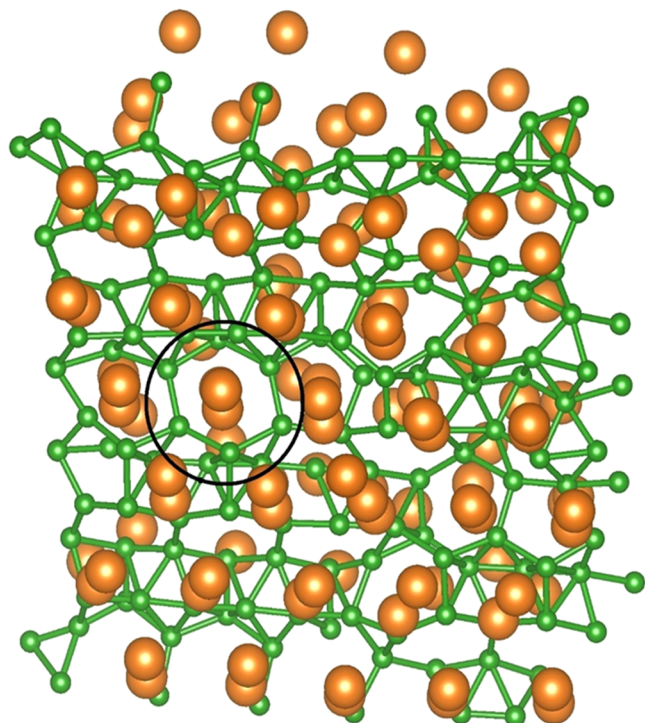


Figure 7. Partial phase change in the most stable Mg-adsorbed striped borophene found using AIRSS. The highlighted portion represents local phase change of Mg-adsorbed striped borophene to Mg-adsorbed hexagonal borophene. The color convention is the same as in Figure 6.

energetics-driven map for developing high-capacity Mg-ion batteries using borophene.

■ ASSOCIATED CONTENT

SI Supporting Information

The Supporting Information is available free of charge at <https://pubs.acs.org/doi/10.1021/acs.jpcc.2c02727>.

Figures for charge density difference of all of the structures, density of states for the most stable structures obtained through the bottom-up structure-searching approach, and AIMD simulation of the most stable AIRSS-found Mg-adsorbed borophene phase (PDF)

■ AUTHOR INFORMATION

Corresponding Author

Santanu Mahapatra – Nano-Scale Device Research Laboratory, Department of Electronic Systems Engineering, Indian Institute of Science (IISc) Bangalore, Bangalore 560012, India; orcid.org/0000-0003-1112-8109; Email: santanu@iisc.ac.in

Authors

Vaishnavi Vishnubhotla – Nano-Scale Device Research Laboratory, Department of Electronic Systems Engineering, Indian Institute of Science (IISc) Bangalore, Bangalore 560012, India

Arnab Kabiraj – Nano-Scale Device Research Laboratory, Department of Electronic Systems Engineering, Indian Institute of Science (IISc) Bangalore, Bangalore 560012, India; orcid.org/0000-0002-7063-0169

Aninda J. Bhattacharyya – Solid State and Structural Chemistry Unit, Indian Institute of Science (IISc) Bangalore,

Bangalore 560012, India; orcid.org/0000-0002-0736-0004

Complete contact information is available at: <https://pubs.acs.org/10.1021/acs.jpcc.2c02727>

Notes

The authors declare no competing financial interest.

■ ACKNOWLEDGMENTS

The authors acknowledge Dr. Sanchali Mitra, Nano-Scale Device Research Laboratory, IISc Bangalore, for valuable inputs regarding AIMD simulation. This work was supported by the Material for Energy Storage (MES) scheme of Technology Mission Division Energy and Water, Department of Science and Technology (DST), Government of India, under Grant DST/TMD/MES/2K18/ 28. A.J.B. also acknowledges the Amrut Mody Chair Professorship for financial support.

■ REFERENCES

- (1) Miao, Y.; Hynan, P.; Von Jouanne, A.; Yokochi, A. Current Li-ion battery technologies in electric vehicles and opportunities for advancements. *Energies* **2019**, *12*, No. 1074.
- (2) Wang, D.; Liu, L. M.; Zhao, S. J.; Hu, Z. Y.; Liu, H. Potential application of metal dichalcogenides double-layered heterostructures as anode materials for Li-ion batteries. *J. Phys. Chem. C* **2016**, *120*, 4779–4788.
- (3) Penev, E. S.; Bhowmick, S.; Sadrzadeh, A.; Yakobson, B. I. Polymorphism of two-dimensional boron. *Nano Lett.* **2012**, *12*, 2441–2445.
- (4) Mannix, A. J.; Zhou, X. F.; Kiraly, B.; Wood, J. D.; Alducin, D.; Myers, B. D.; Guisinger, N. P.; et al. Synthesis of borophenes: Anisotropic, two-dimensional boron polymorphs. *Science* **2015**, *350*, 1513–1516.
- (5) Li, W.; Kong, L.; Chen, C.; Gou, J.; Sheng, S.; Zhang, W.; Wu, K.; et al. Experimental realization of honeycomb borophene. *Sci. Bull.* **2018**, *63*, 282–286.
- (6) Wang, Z. Q.; Lü, T. Y.; Wang, H. Q.; Feng, Y. P.; Zheng, J. C. Review of borophene and its potential applications. *Front. Phys.* **2019**, *14*, No. 33403.
- (7) Liu, Y.; Penev, E. S.; Yakobson, B. I. Probing the synthesis of two-dimensional boron by first-principles computations. *Angew. Chem., Int. Ed.* **2013**, *52*, 3156–3159.
- (8) Jiang, H. R.; Lu, Z.; Wu, M. C.; Ciucci, F.; Zhao, T. S. Borophene: a promising anode material offering high specific capacity and high-rate capability for lithium-ion batteries. *Nano Energy* **2016**, *23*, 97–104.
- (9) Kabiraj, A.; Bhattacharyya, A. J.; Mahapatra, S. Thermodynamic Insights into Polymorphism-Driven Lithium-Ion Storage in Monolayered 2D Materials. *J. Phys. Chem. Lett.* **2021**, *12*, 1220–1227.
- (10) Schmuch, R.; Wagner, R.; Hörpel, G.; Placke, T.; Winter, M. Performance and cost of materials for lithium-based rechargeable automotive batteries. *Nat. Energy* **2018**, *3*, 267–278.
- (11) Yabuuchi, N.; Komaba, S. Recent research progress on iron- and manganese-based positive electrode materials for rechargeable sodium batteries. *Sci. Technol. Adv. Mater.* **2014**, *15*, No. 043501.
- (12) Ladha, D. G. A review on density functional theory–based study on two-dimensional materials used in batteries. *Mater. Today Chem.* **2019**, *11*, 94–111.
- (13) Kabiraj, A.; Mahapatra, S. High-throughput assessment of two-dimensional electrode materials for energy storage devices. *Cell Rep. Phys. Sci.* **2022**, *3*, No. 100718.
- (14) Li, J.; Tritsarlis, G. A.; Zhang, X.; Shi, B.; Yang, C.; Liu, S.; Lu, J.; et al. Monolayer honeycomb borophene: A promising anode material with a record capacity for lithium-ion and sodium-ion batteries. *J. Electrochem. Soc.* **2020**, *167*, No. 090527.
- (15) Mortazavi, B.; Rahaman, O.; Ahzi, S.; Rabczuk, T. Flat borophene films as anode materials for Mg, Na or Li-ion batteries

with ultra high capacities: A first-principles study. *Appl. Mater. Today* **2017**, *8*, 60–67.

(16) Mortazavi, B.; Dianat, A.; Rahaman, O.; Cuniberti, G.; Rabczuk, T. Borophene as an anode material for Ca, Mg, Na or Li ion storage: a first-principle study. *J. Power Sources* **2016**, *329*, 456–461.

(17) Bahari, Y.; Mortazavi, B.; Rajabpour, A.; Zhuang, X.; Rabczuk, T. Application of two-dimensional materials as anodes for rechargeable metal-ion batteries: A comprehensive perspective from density functional theory simulations. *Energy Storage Mater.* **2021**, *35*, 203–282.

(18) Makaremi, M.; Mortazavi, B.; Singh, C. V. 2D Hydrogenated graphene-like borophene as a high capacity anode material for improved Li/Na ion batteries: A first principles study. *Mater. Today Energy* **2018**, *8*, 22–28.

(19) George, C.; Morris, A. J.; Modarres, M. H.; De Volder, M. Structural evolution of electrochemically lithiated MoS₂ nanosheets and the role of carbon additive in Li-ion batteries. *Chem. Mater.* **2016**, *28*, 7304–7310.

(20) Kabiraj, A.; Mahapatra, S. High-throughput first-principles-calculations based estimation of lithium-ion storage in monolayer rhenium disulfide. *Commun. Chem.* **2018**, *1*, No. 81.

(21) Wang, D.; Liu, Y.; Meng, X.; Wei, Y.; Zhao, Y.; Pang, Q.; Chen, G. Two-dimensional VS₂ monolayers as potential anode materials for lithium-ion batteries and beyond: first-principles calculations. *J. Mater. Chem. A* **2017**, *5*, 21370–21377.

(22) Kabiraj, A.; Mahapatra, S. Intercalation-Driven Reversible Switching of 2D Magnetism. *J. Phys. Chem. C* **2020**, *124*, 1146–1157.

(23) Liu, J.; Zhang, C.; Xu, L.; Ju, S. Borophene as a promising anode material for sodium-ion batteries with high capacity and high-rate capability using DFT. *RSC Adv.* **2018**, *8*, 17773–17785.

(24) Kresse, G.; Hafner, J. Ab initio molecular dynamics for liquid metals. *Phys. Rev. B* **1993**, *47*, No. 558.

(25) Kresse, G.; Hafner, J. Ab initio molecular-dynamics simulation of the liquid-metal–amorphous-semiconductor transition in germanium. *Phys. Rev. B* **1994**, *49*, No. 14251.

(26) Kresse, G.; Furthmüller, J. Efficient iterative schemes for ab initio total-energy calculations using a plane-wave basis set. *Phys. Rev. B* **1996**, *54*, No. 11169.

(27) Kresse, G.; Furthmüller, J. Efficiency of ab-initio total energy calculations for metals and semiconductors using a plane-wave basis set. *Comput. Mater. Sci.* **1996**, *6*, 15–50.

(28) Kresse, G.; Joubert, D. From ultrasoft pseudopotentials to the projector augmented-wave method. *Phys. Rev. B* **1999**, *59*, No. 1758.

(29) Perdew, J. P.; Burke, K.; Ernzerhof, M. Generalized gradient approximation made simple. *Phys. Rev. Lett.* **1996**, *77*, 3865.

(30) Grimme, S.; Antony, J.; Ehrlich, S.; Krieg, H. A consistent and accurate ab initio parametrization of density functional dispersion correction (DFT-D) for the 94 elements H–Pu. *J. Chem. Phys.* **2010**, *132*, No. 154104.

(31) Jing, Y.; Zhou, Z.; Cabrera, C. R.; Chen, Z. Metallic VS₂ monolayer: a promising 2D anode material for lithium-ion batteries. *J. Phys. Chem. C* **2013**, *117*, 25409–25413.

(32) Su, J.; Pei, Y.; Yang, Z.; Wang, X. Ab initio study of graphene-like monolayer molybdenum disulfide as a promising anode material for rechargeable sodium ion batteries. *RSC Adv.* **2014**, *4*, 43183–43188.

(33) Kulish, V. V.; Malyi, O. I.; Persson, C.; Wu, P. Phosphorene as an anode material for Na-ion batteries: a first-principles study. *Phys. Chem. Chem. Phys.* **2015**, *17*, 13921–13928.

(34) Oganov, A. R.; Glass, C. W. Crystal structure prediction using ab initio evolutionary techniques: Principles and applications. *J. Chem. Phys.* **2006**, *124*, No. 244704.

(35) Lyakhov, A. O.; Oganov, A. R.; Stokes, H. T.; Zhu, Q. New developments in evolutionary structure prediction algorithm USPEX. *Comput. Phys. Commun.* **2013**, *184*, 1172–1182.

(36) Oganov, A. R.; Lyakhov, A. O.; Valle, M. How Evolutionary Crystal Structure Prediction Works- and Why. *Acc. Chem. Res.* **2011**, *44*, 227–237.

(37) Pickard, C. J.; Needs, R. J. Ab initio random structure searching. *J. Phys.: Condens. Matter* **2011**, *23*, No. 053201.

(38) Nosé, S. A unified formulation of the constant temperature molecular dynamics methods. *J. Chem. Phys.* **1984**, *81*, 511–519.

(39) Hoover, W. G. Canonical dynamics: Equilibrium phase-space distributions. *Phys. Rev. A* **1985**, *31*, No. 1695.

(40) Manz, T. A.; Limas, N. G. Introducing DDEC6 atomic population analysis: part 1. Charge partitioning theory and methodology. *RSC Adv.* **2016**, *6*, 47771–47801.

(41) Limas, N. G.; Manz, T. A. Introducing DDEC6 atomic population analysis: part 2. Computed results for a wide range of periodic and nonperiodic materials. *RSC Adv.* **2016**, *6*, 45727–45747.

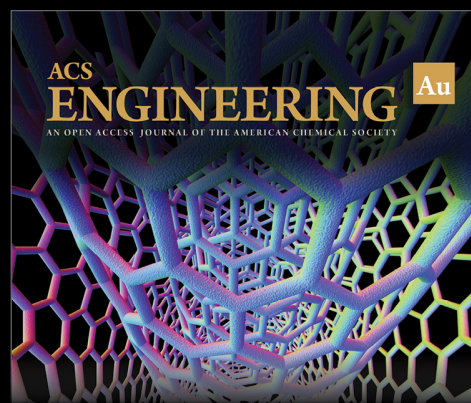
(42) Manz, T. A.; Sholl, D. S. Improved atoms-in-molecule charge partitioning functional for simultaneously reproducing the electrostatic potential and chemical states in periodic and nonperiodic materials. *J. Chem. Theory Comput.* **2012**, *8*, 2844–2867.

(43) Manz, T. A.; Gabaldon Limas, N. Chagemol Program for Performing DDEC Analysis, version 3.5, 2017. <http://ddec.sourceforge.net>.

(44) Momma, K.; Izumi, F. VESTA 3 for three-dimensional visualization of crystal, volumetric and morphology data. *J. Appl. Crystallogr.* **2011**, *44*, 1272–1276.

(45) Putungan, D. B.; Lin, S. H.; Kuo, J. L. Metallic VS₂ monolayer polytypes as potential sodium-ion battery anode via ab initio random structure searching. *ACS Appl. Mater. Interfaces* **2016**, *8*, 18754–18762.

(46) Feng, B.; Zhang, J.; Zhong, Q.; Li, W.; Li, S.; Li, H.; Wu, K.; et al. Experimental realization of two-dimensional boron sheets. *Nat. Chem.* **2016**, *8*, 563–568.



Editor-in-Chief: **Prof. Shelley D. Minteer**, University of Utah, USA



Deputy Editor:

Prof. Vivek Ranade

University of Limerick, Ireland

Open for Submissions 

pubs.acs.org/engineeringau

 **ACS Publications**
Most Trusted. Most Cited. Most Read.